

Monomeric Three-Coordinate N-Heterocyclic Carbene Nickel(I) Complexes: Synthesis, Structures, and Catalytic Applications in Cross-Coupling Reactions

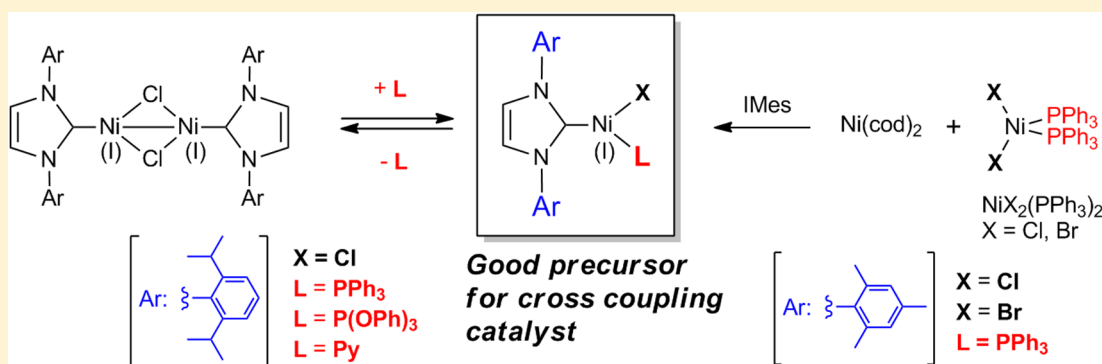
Kouki Matsubara,^{*,†} Yukino Fukahori,^{†,‡} Takahiro Inatomi,[†] Saeko Tazaki,[†] Yuji Yamada,[†] Yuji Koga,[†] Shinji Kanegawa,[§] and Toshikazu Nakamura[‡]

[†]Department of Chemistry, Fukuoka University, 8-19-1 Nanakuma, Fukuoka 814-0180, Japan

[‡]Institute for Molecular Science, Myodaiji, Okazaki, Aichi 444-8585, Japan

[§]Institute for Materials Chemistry and Engineering, Kyushu University, 744 Motoooka, Nishi-ku, Fukuoka 819-0395, Japan

Supporting Information



ABSTRACT: A series of three-coordinate monovalent nickel halide complexes bearing N-heterocyclic carbene (NHC) ligands, i.e., NiCl(IPr)(L) [L = pyridine, P(OPh)₃, bis(diphenylphosphino)butane (dppb), IPr = 1,3-bis(2,6-diisopropylphenyl)imidazol-2-ylidene], NiX(IMes)(PPh₃) (X = Cl and Br, IMes = 1,3-bis(mesityl)imidazol-2-ylidene), were prepared. The complexes were identified using NMR spectroscopy, superconducting quantum interference device (SQUID), and X-ray crystallography. Additionally, ESR spectra of NiCl(IPr)(pyridine) were taken in toluene. These complexes had three-coordinate Y-shaped geometries in both the solid and solution states. The compounds containing IPr showed equilibrium between the monomeric and dimeric forms, with liberation of ligands. Addition of 1,2-bis(diphenylphosphino)ethane and 1,3-bis(diphenylphosphino)propane to the dinickel(I) IPr complex instead of dppb resulted in heterolytic cleavage to nickel(0) and nickel(II) species. Catalysis of Suzuki cross-coupling and Buchwald–Hartwig amination of aryl bromide using the complexes was investigated. The efficiencies in the amination of aryl bromide depended strongly on the additional donor ligands.

INTRODUCTION

Organonickel-catalyzed organic transformations have been widely studied in recent decades, and many useful reactions have been discovered.¹ A general feature of nickel-mediated reactions is oxidation of a zerovalent species to a nickel(II) species, which is then reduced to complete the catalytic cycle. However, zerovalent nickel species, unlike zerovalent palladium species, are generally unstable; therefore the development of efficient methods for reduction to nickel(0) is important in developing efficient catalytic processes.² On the other hand, monovalent nickel species have recently been reported in useful cross-coupling reactions,³ and well-defined nickel(I) complexes have been shown to mediate cross-coupling reactions of aryl and alkyl halides;⁴ for example, Vicić et al. reported that a terpyridine-stabilized nickel(I) complex catalyzed the Negishi coupling of alkyl halides.⁵ These monovalent nickel-catalyzed processes have advantages over the usual nickel(0) catalysts for

the following reasons: (1) reduction to nickel(I) species is easier than reduction to nickel(0) in catalytic cycles; (2) the unpaired electron weakens the nickel–ligand bonding interactions, resulting in easier elimination of ligand and/or the product in catalysis than the diamagnetic nickel species.⁴ Therefore, the development of nickel(I)-catalyzed organic reactions and new catalytic systems is important in both organic and organometallic chemistry.

Examples of catalysts starting from well-defined nickel(I) precursors have rarely been reported,⁴ although many examples of monovalent nickel complexes are known.⁶ This is because nickel(I) compounds are frequently thermally unstable and disproportionate to form nickel(0) and nickel(II) compounds. They are also extremely unstable in air and generally form

Received: May 25, 2016

oxidized compounds. Bulky N-heterocyclic carbene (NHC) ligands thermally stabilize nickel(I) species in catalysis.⁴ Among such nickel(I) complexes, monovalent nickel chloride bearing two IPr ligands, i.e., Ni(IPr)₂Cl, where IPr is 1,3-bis(2,6-diisopropylphenyl)imidazol-2-ylidene, is in equilibrium with dinuclear nickel(I) chloride, [Ni(IPr)]₂(μ-Cl)₂ (**1**), with elimination of one IPr ligand.^{4a} This prompted us to add PPh₃ as a two-electron-donor ligand to **1**, prepared by another method,⁷ resulting in efficient generation of a three-coordinate Y-shaped monomeric nickel(I) complex, Ni(IPr)Cl(PPh₃) (**2a**).⁸ Complex **2a** was more air-stable than **1**, and it catalyzed Kumada–Tamao–Corriu coupling and Buchwald–Hartwig aminations of aryl bromides more efficiently than did **1** and Ni(IPr)₂Cl. PPh₃ is easily eliminated from **2a** to form an unsaturated and highly active, monomeric two-coordinate species, Ni(IPr)Cl, or the dimeric nickel(I) complex **1** because of the strong *trans* effect of the NHC ligand,⁹ and the stable resting state, with recoordination of PPh₃, stabilizes the catalytic system. Excess PPh₃ did not deactivate the process and did not compete with the substrates for coordination to nickel. Our preliminary results showed that Ni(IPr)₂Cl reduction with a Grignard reagent readily forms a zerovalent complex Ni(IPr)₂, without elimination of IPr, whereas **2a** eliminates phosphine in conjunction with the Grignard reagent to form a dimeric nickel(I) transmetalation product.⁸ The introduction of other donor ligands, including other phosphines and pyridine derivatives, to **2** could be used to control the activity and stability of the monovalent nickel complex **2**.

A large variety of bulky NHC ligands have been designed and built for use in catalysts.¹⁰ We focused on the structural differences between IPr and 1,3-bis(mesityl)imidazol-2-ylidene (IMes); the different steric effects around the metal centers result in clear differences between their reactivities and stabilities. Monovalent nickel species bearing an IPr or IMes ligand differ significantly; for example, preparation of an IMes analogue of the dimeric nickel(I) compound **1** is impossible. This indicates that the monomeric IMes analogue of **2** and the IPr complex **2** cannot be synthesized using the same method. However, several nickel(I) NHC complexes have been prepared from Ni(cod)₂ and NiX₂L₂ (X = halogen, L = 1,2-dimethoxyethane or triphenylphosphine) in the presence of an NHC.^{7,11}

In this study, we prepared a series of nickel(I) complexes bearing IPr and IMes and various two-electron-donor ligands. These compounds were characterized using spectroscopy, superconducting quantum interference device (SQUID) measurements, and X-ray crystallography. The catalytic activities of the monomeric nickel(I) complexes in the Suzuki coupling and Buchwald–Hartwig amination of aryl bromides were compared.

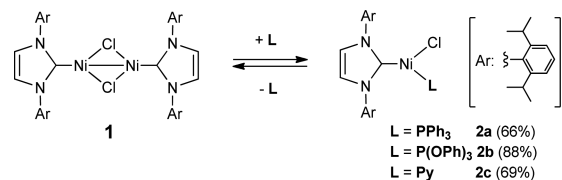
RESULTS AND DISCUSSION

Preparation of Monomeric Nickel(I) NHC Complexes.

The IPr complexes **2** were synthesized from dimeric complex **1** and two-electron-donor ligands (Scheme 1). The P(OPh)₃ analogue Ni(IPr)Cl(P(OPh)₃) (**2b**) was readily isolated in 88% yield as red-orange crystals. Addition of pyridine to a solution of **1** afforded Ni(IPr)Cl(pyridine) (**2c**), in which only one molecule of pyridine was coordinated to nickel, in 69% yield upon recrystallization.

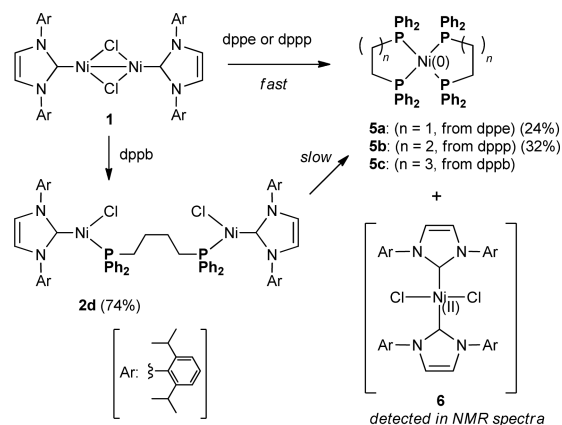
Bisphosphines also reacted with **1**. However, the addition of 1,2-bis(diphenylphosphino)ethane (dppe) or 1,3-bis(diphenylphosphino)propane (dppp) gave not the expected

Scheme 1. Preparation of Mononickel(I) IPr Complexes



monovalent nickel complex **2** but mixtures containing zerovalent nickel complexes Ni(dppe)₂ (**5a**)¹² or Ni(dppp)₂ (**5b**).¹³ Divalent complex Ni(IPr)₂Cl₂ (**6**) was also detected as the product in the crude reaction mixture (see the SI). Zerovalent complexes **5a** and **5b** were isolated as crystals in 24% and 32% yield, respectively, although **6** could not be isolated. It should be noted that when 1,4-bis(diphenylphosphino)butane (dppb), in which the methylene chain is one carbon longer than dppp, was used as the ligand, the dinickel(I) dppb complex [Ni(IPr)Cl]₂(dppb) (**2d**) was successfully obtained in 74% yield upon recrystallization (Scheme 2). However, the complex **2d** rearranged slowly in

Scheme 2. Reaction of **1** with Bisphosphines

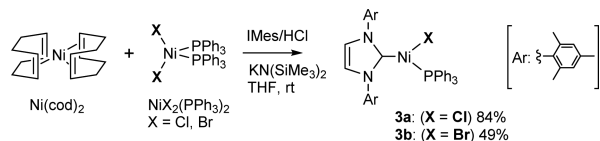


the benzene-*d*₆ solution in a day to form a mixture of the zerovalent complex Ni(dppb)₂¹⁴ (**5c**), suggesting that disproportionation occurred via formation of the dinickel(I) intermediate **2** even in the reactions with dppe and dppp. Aggregation of the paramagnetic nickel(I) centers as a result of the short methylene linkages in dppe and dppp may enable facile electron transfer from one of the nickel(I) atoms to the other, generating nickel(0) and nickel(II) species, whereas the longer chain in dppb makes electron transfer slower. If electron transfer from nickel(I) to nickel(I) occurred through the bonding interaction, the dimeric nickel(I) complex **1** would easily heterolytically split into nickel(0) and nickel(II) species; however, this never occurs. Through-space electron transfer between the two nickel(I) centers closely linked by the bidentate ligands may be necessary in the disproportionation. This is a rare and significant example of the electron transfer rate being controlled by the distance between two monovalent nickel centers (Ni–P–(CH₂)₃–P–Ni and Ni–P–(CH₂)₄–P–Ni).¹⁵ Complex **2d** was not used as a catalyst in the following catalytic studies, because the complex **5c** can be formed in situ under the catalytic conditions.

As noted above, the smaller IMes ligand did not provide the analogue of the dimeric nickel(I) IPr complex **1**, because the bulky ligand, i.e., IPr, is probably desirable to stabilize the

coordinatively unsaturated dimer complex kinetically. The corresponding monomeric IMes analogues of **2** were therefore synthesized using Whittlesey's method.¹¹ Ni(cod)₂, NiX₂(PPh₃)₂ (X = Cl and Br), and IMes/HCl were mixed in the presence of KN(SiMe₃)₂ as a base, resulting in in situ generation of the free carbene, at room temperature. The reaction efficiently afforded the expected Ni(IMes)X(PPh₃) (**3a**: X = Cl; **3b**: X = Br) in 84% and 49% yields by recrystallization (Scheme 3). These IMes analogues **3** were very unstable in air, but the bromide complex **3b** was more stable than the chloride counterpart **3a**.

Scheme 3. Preparation of Mononickel(I) IMes Complexes



Broad paramagnetic signals were observed in the ¹H NMR spectra of the monomeric nickel(I) compounds **2b–d**, **3a**, and **3b** at around δ 1–14, similar to those for **2a** (see the SI). As previously reported, an unpaired electron is delocalized only on the nickel d-orbital, providing sharp solvent signals in the ¹H NMR spectra.^{4a} DFT calculations also supported these results, as described below.

When crystals of **2a** and **2b** were dissolved in benzene-*d*₆, the dimeric compound **1** was generated in situ with liberation of the free ligand and was detected in the ¹H NMR spectrum. Addition of extra portions (2–5 equiv) of the ligand to the solutions resulted in the disappearance of **1**, indicating that there is equilibrium in solution between the monomeric and dimeric nickel(I) complexes in the presence of the donor ligands. The relative ratios of **1**:**2a–c** in equilibrium depended on the ligand: pyridine (**2c**) > PPh₃ (**2a**) > P(OPh)₃ (**2b**).¹⁶ This trend is related to the π-acceptor abilities of these ligands, as expected. In contrast to the IPr complexes **2**, the diamagnetic dimeric complexes [Ni(IMes)]₂(μ-X)₂ were not observed when crystals of **3a** and **3b** were dissolved in benzene-*d*₆. When 5 equiv of pyridine was added to a solution of **2c**, the ¹H NMR spectrum showed no sharp signals assignable to free pyridine, suggesting fast equilibrium between coordination and elimination of pyridine molecules. Although we have no direct information on the solution structure, we assume that elimination of pyridine gives a 13-electron linear structure without coordination of pyridine or formation of a tetracoordinate 17-electron complex, Ni(IPr)Cl(pyridine)₂, with tetrahedral geometry around the nickel(I) center.

The spin states of the series of monomeric nickel(I) complexes were investigated based on SQUID measurements of **2b–d**. It was previously reported that **2a** has *S* = 1/2 ($\chi_{\text{mol}}T$ = 0.44 cm³ K mol⁻¹ at -263 °C, where χ_{mol} is molar magnetic susceptibility) and a three-coordinate Y-shaped 15-electron structure.⁸ The spin quantum numbers of the other complexes were also 1/2 [$\chi_{\text{mol}}T$ = 0.35 (**2b**), 0.52 (**2c**), 0.34 (**2d**, per nickel atom) at -253 °C] (see the SI). Any magnetic interaction between nickel(I) centers in the dinuclear complex **2d** was not observed, even at -268 °C, because the distance between the two nickel atoms, which was estimated from the crystal structure (shown below), was too long (ca. 8.30 Å) for them to interact with each other. The theoretical value of $\chi_{\text{mol}}T$ is 0.375 cm³ K mol⁻¹ when *S* = 1/2; therefore that of **2c** is

slightly higher than the theoretical value and also of those of the other complexes (Figure 1a). The ESR spectrum of **2c** in

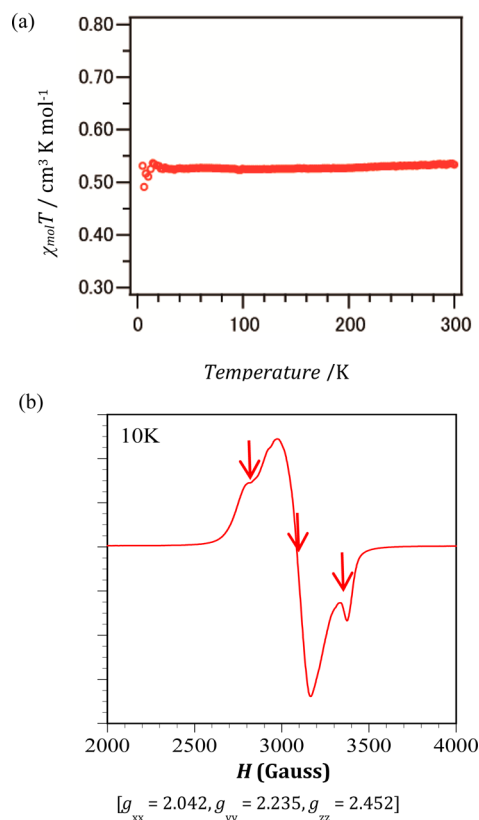


Figure 1. (a) $\chi_{\text{mol}}T$ versus temperature plots of **2c** and (b) frozen solution ESR spectrum of **2c** at 10 K (-263 °C) in dilute toluene.

toluene at -263 °C showed three-axial anisotropy [$g_{xx} = 2.042$, $g_{yy} = 2.235$, $g_{zz} = 2.452$] (Figure 1b). The $\chi_{\text{mol}}T$ calculated from these *g* values is 0.47, which is almost in agreement with that from the SQUID results.

Figure 2 shows the crystal structures of **2b**, **2c**, **2d**, **3a**, and **3b**. Representative bond lengths and angles around the nickel atom, including those for **2a**, are listed in Table 1. The sum of the angles around the nickel atom was almost 360° in each complex, indicating planar three-coordinate geometries. The Ni–C(carbene) and Ni–Cl distances and the angles around the nickel atom did not differ between **2** and **3**, indicating that the differences between the shapes and sizes of the NHC ligands did not affect the structures around the nickel atom. On the basis of the π-acceptor ability of the phosphorus ligand, the P–Ni bond distance in **2b** was 0.1 Å shorter than that in **2a**. The Cl–Ni–C(carbene) angle in **2c**, which contains pyridine, is 142.1(1)°, which is much larger than those for the other phosphine complexes, i.e., 131–134°. The Ni–N(pyridine) bond distance was 2.200(3) Å, which is significantly longer than the usual nickel–nitrogen σ-bond distances, i.e., ca. 2.0 Å.¹⁷ Delocalization of the unpaired electron in the Ni–N(pyridine) σ*-orbital was negligible (2.5%) (calculated below); therefore this elongation must be ascribed to other reasons. This weak interaction may stretch the Cl–Ni–C(carbene) hinge.

Theoretical Studies. The distribution of the single-electron-occupied molecular orbital (SOMO) was investigated by performing single-point DFT calculations at the fixed geometries given by the crystallographic coordinates of **2a–c**

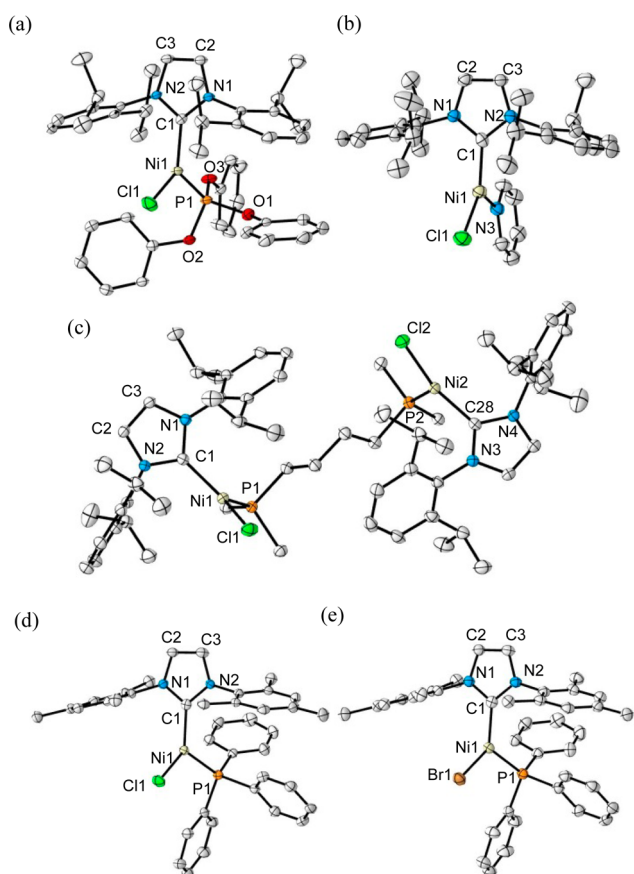


Figure 2. ORTEP drawings of nickel(I) complexes: (a) **2b**, (b) **2c**, (c) **2d**, (d) **3a**, and (e) **3b** (50% probability thermal ellipsoids). All hydrogen atoms are omitted. Three THF molecules and four phenyl rings on **dpbb** in **2d** and two THF molecules in **3a** and **3b** are also omitted for clarity.

and **3a** with the B3LYP functional and 6-31G(d,p) basis set (Figure 3). In complex **2a**, the unpaired electron is localized mainly on the nickel d-orbital (51.4%) and the chlorine–nickel π^* -orbital (11.9%). It also forms a phosphorus–nickel σ^* -bond (12.4%).^{4c} The distribution in **2b** was similar to that in **2a**: nickel d-orbital (47.8%), Ni–Cl π^* -orbital (13.8%), and Ni–P σ -orbital (12.3%). In contrast, in **2c**, the unpaired electron is located mainly on nickel (80.7%), and the values for the Ni–Cl and Ni–N bonds are 4.5% and 2.5%, respectively. Generally, the nonbonding orbital energy of pyridine is lower than that of phosphorus; therefore the energy gap between nickel and nitrogen is larger than that between nickel and phosphorus, weakening the nickel–pyridine interactions, including donation

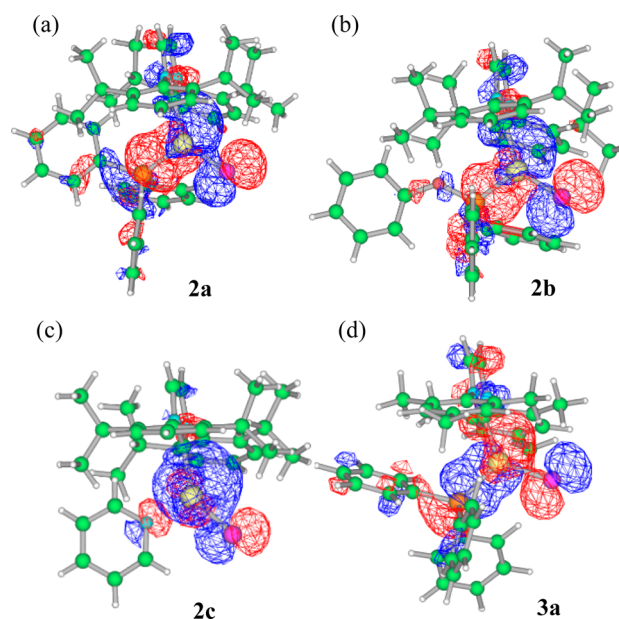


Figure 3. SOMOs (red and blue mesh; density isosurface value of 0.02 au) in (a) **2a**, (b) **2b**, (c) **2c**, and (d) **3a** obtained from single-point DFT calculations at the B3LYP/6-31G(d,p) level using crystallographic coordinates (nickel, yellow; orange, phosphorus; purple, chlorine; nitrogen, light blue; carbon, green).

and π -back-donation, compared with those in the Ni–P bond. There were no conspicuous differences between the IPr complex **2a** and the corresponding IMes analogue **3a**, suggesting that different substituents on the NHC ligands do not affect the electronic structures of these complexes.

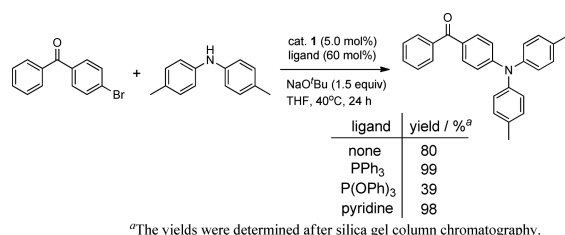
Catalytic Applications in Buchwald–Hartwig Amination and Suzuki–Miyaura Cross-Coupling Reactions.

The obtained monovalent nickel compounds were used in catalytic cross-coupling reactions. Their catalytic activities were compared by performing Buchwald–Hartwig aminations of bromobenzophenone with diphenylamine, under reaction conditions using **2a** as the catalyst, similar to those previously reported.⁸ Scheme 4 shows the reaction protocol and yields of the triarylamine products. Excess amounts of the two-electron-donor ligands [PPh₃, P(OPh)₃, and pyridine] were added to 5 mol % of **1** to generate the corresponding monomeric nickel(I) complexes **2a**, **2b**, and **2c** in situ. The substrates were then added, and the mixture was stirred at 40 °C for 24 h in THF. The products were isolated after silica gel column chromatography. The ligand strongly affected the product yields, which were 99% for PPh₃, 39% for P(OPh)₃, and 98% for pyridine. The smallest ligand, i.e., pyridine, did not inhibit interactions of

Table 1. Representative Bond Distances and Angles for **2a**, **2b**, **2c**, **2d**, **3a**, and **3b**

	2a (Y = P)	2b (Y = P)	2c (Y = N)	2d (Y = P)	3a (X = Cl)	3b (X = Br)
Bond Lengths (Å)						
Ni(1)–C(1)	1.930(3)	1.928(3)	1.909(4)	1.937(2), 1.939(2)	1.938(4)	1.949(3)
Ni(1)–X(1)	2.1786(9)	2.1545(9)	2.201(1)	2.1973(7), 2.1994(7)	2.188(1)	2.3178(6)
Ni(1)–Y(1)	2.201(1)	2.1170(6)	2.200(3)	2.2042(6), 2.2006(6)	2.205(1)	2.2051(9)
Bond Angles (deg)						
X(1)–Ni(1)–C(1)	134.2(1)	134.29(6)	142.1(1)	132.29(6), 136.99(6)	132.8(1)	131.03(9)
Y(1)–Ni(1)–C(1)	112.1(1)	109.41(6)	107.2(1)	112.79(6), 111.71(6)	111.6(1)	112.76(9)
X(1)–Ni(1)–Y(1)	113.31(4)	116.30(3)	110.73(9)	114.37(3), 110.72(3)	115.31(5)	115.95(3)
\sum_{Ni}	359.5(1)	360.00(6)	360.0(1)	359.45(6), 359.42(6)	359.7(1)	359.74(9)

Scheme 4. Triarylamine Formation via Buchwald–Hartwig Amination

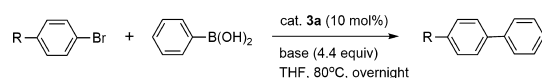


the substrates with nickel. Pyridine can be easily eliminated from **2c** to generate the active form **1**, whereas little P(OPh)₃ is eliminated from **2b**, preventing generation of the active species. Interestingly, PPh₃ adequately controls the concentration of **1** and stabilizes the unstable active species to form the monomeric complex as the resting state.

In our preliminary research, a series of IPr complexes of nickel(I) were inactive in the Suzuki cross-coupling reactions of aryl halides. In general, the Suzuki cross-coupling reaction does not require steric hindrance derived from bulky ligands on metal centers,¹⁸ in contrast to Buchwald–Hartwig amination, which does require bulky ligands.¹⁹ In this case, the bulkiness of the ligand is critical in inhibiting the reaction: the IMes complex is catalytically active, but the IPr complex is not. Louie et al. reported monovalent-nickel-catalyzed Suzuki coupling of aryl halides using a bis(IMes) complex of nickel(I), [NiCl(IMes)₂].^{4b} Here, we used the analogous complex **3a**, containing PPh₃ instead of IMes.

We used an activated aryl bromide, 4-bromobenzophenone, in cross-coupling with phenylboronic acid in the presence of the monovalent nickel chloride complex **3a** (10 mol %) (Table 2). Base screening showed that using NaO^tBu and KO^tBu

Table 2. Suzuki–Miyaura Cross-Coupling Reactions of Aryl Bromides with Phenylboronic Acid



entry	R–	base	solvent	yield/% ^a
1	PhCO–	NaO ^t Bu	toluene	54
2	PhCO–	KO ^t Bu	toluene	65
3	PhCO–	K ₃ PO ₄	toluene	66
4	PhCO–	K ₂ CO ₃	toluene	79
5	PhCO–	Cs ₂ CO ₃	toluene	88
6	PhCO–	Cs ₂ CO ₃	THF	68
7	PhCO–	Cs ₂ CO ₃	CPME	72
8	CH ₃ O–	Cs ₂ CO ₃	toluene	45

^aThe yields were determined with GC-MS. Calibration was carried out using a standard sample of 4,4'-dimethoxybiphenyl.

(entries 1 and 2) and potassium phosphonate and carbonate (entries 3 and 4) provided moderate to good yields (54–79%) of the cross-coupling products. Cesium carbonate was the best base and afforded the product in 88% yield (entry 5). Toluene was a better solvent than THF and cyclopentyl methyl ether (CPME) (entries 6 and 7). When the less active bromoanisole was used as the substrate, the yield after 4 h was moderate (45%; entry 8).^{4b}

CONCLUSION

In summary, we have developed synthetic methods for a series of monovalent nickel complexes bearing mixed ligands, namely, bulky NHCs and other two-electron-donor ligands. The complex structures were determined using SQUID, ESR, and X-ray crystallography. The chemical structures of the two-electron-donor ligands affected the stabilities, SOMO distributions, and catalytic activities of the corresponding nickel(I) complexes. Pyridine weakly coordinates to nickel(I) and is easily liberated to form the dimeric complex, whereas P(OPh)₃ strongly binds to nickel(I) and stabilizes the monomeric form. The monomeric complexes Ni(IPr)Cl(L) were not thermally stable when diphosphines bridged with a three- or two-carbon unit, e.g., dppp or dppe, were introduced, and mixtures of zerovalent and divalent nickel complexes were obtained, probably because of easy electron transfer and subsequent disproportionation. However, a dppb complex of nickel(I) was successfully isolated and characterized, although it was slowly transformed into a mixture of nickel(0) and nickel(II) species. The bulky NHCs IPr and IMes do not affect the electronic structures of the monomeric nickel(I) complexes, but the dimeric IPr complex [Ni(IPr)]₂(μ-Cl)₂ is much more stable than its IMes analogue. Monovalent nickel complexes bearing both IPr and IMes ligands are active in cross-coupling reactions of aryl bromides. Buchwald–Hartwig aminations using the monovalent nickel(I) IPr complexes as catalysts proceeded efficiently to yield triarylamines. The IPr complexes did not catalyze the Suzuki cross-coupling reactions of aryl halides, although the active IMes analogues did. These small differences derived from the NHC ligand structures help precisely control catalytic processes. Mechanistic studies of these cross-coupling reactions using monovalent nickel complexes and the development of air-stable nickel(I) catalyst precursors are now in progress.

EXPERIMENTAL SECTION

General Procedures. All experiments were performed in an inert gas atmosphere using standard Schlenk techniques and a glovebox (MBraun UNILab), unless otherwise stated. THF, hexane, toluene, and benzene-*d*₆ were distilled from benzophenone ketyl and stored in a nitrogen atmosphere with 4A molecular sieves. Chloroform-*d* was distilled from CaH₂ and stored in a nitrogen atmosphere. Other reagents were used as received or distilled just before use if possible. ¹H NMR spectra were obtained at room temperature using a Varian Mercury Y Plus 400 MHz spectrometer. Chemical shifts (δ) were recorded in parts per million from the solvent signal. GC-MS was performed using an Agilent 6890N gas chromatograph coupled with a JEOL JMS-GC mate II mass spectrometer. A 60 m InertCap 1 column (0.25 mm i.d., 0.25 μm film thickness) was used, and the injection temperature was 270 °C. Elemental analysis was performed using a Yanaco CHN Corder MT-5 autosampler. CW X-band ESR spectra were measured by a Bruker E500 ESR spectrometer. The measurement temperature was controlled by an Oxford ESR900 cryostat and an ITC503 temperature controller in the temperature range from 4 to 296 K. The *g* value was calibrated using a NMR teslameter. The magnetic properties of the materials were investigated using a Quantum Design MPMS-5S SQUID magnetometer. Column chromatography of organic products was performed using silica gel (Kanto Kagaku, silica gel 60 N, spherical, neutral). The NHC was prepared from the imidazolium salts using the published method.²⁰ The monovalent dinuclear nickel IPr complex **1** was prepared as described in the literature.²¹

[NiCl(P(OPh)₃)(IPr)] (2b). In a glovebox, [(μ-Cl)(IPr)Ni]₂ (**1**; 0.03 mmol, 30 mg), P(OPh)₃ (0.06 mmol, 15 μL), and THF (0.5 mL) were added to a 5 mL screw-capped tube. After the compounds had dissolved, hexane (1.5 mL) was slowly added and the solution was

cooled to $-30\text{ }^{\circ}\text{C}$. Colorless crystals of **2b** were obtained after removal of the liquid and washing with a small amount of hexane (85 mg, 88% yield). $^1\text{H NMR}$ (C_6D_6): δ 1.62 (bs), 4.13 (bs), 6.94 (bs), 7.68 (bs), 8.09–8.31 (bs), 10.44 (bs). Anal. Calcd (%) for $\text{C}_{45}\text{H}_{51}\text{N}_2\text{O}_3\text{PClNi}$: C, 68.16; H, 6.48; N, 3.53. Found: C, 68.63; H, 6.59; N, 3.57.

[NiCl(pyridine)(IPr)] (2c). In a glovebox, $[(\mu\text{-Cl})(\text{IPr})\text{Ni}]_2$ (**1**; 0.03 mmol, 30 mg), pyridine (0.12 mmol, 9.6 μL), and THF (0.5 mL) were added to a 5 mL screw-capped tube. After the compounds had dissolved, hexane (1.5 mL) was slowly added and the solution was cooled to $-30\text{ }^{\circ}\text{C}$. Vermillion crystals of **2c** were obtained after removal of the liquid and washing with a small amount of hexane (24 mg, 69% yield). $^1\text{H NMR}$ (C_6D_6): δ 1.18 (bs), 1.75 (bs), 2.48 (bs), 3.08 (bs), 6.37 (bs), 6.95 (bs), 10.7 (bs). Anal. Calcd (%) for $\text{C}_{32}\text{H}_{41}\text{N}_3\text{ClNi}$: C, 68.41; H, 7.36; N, 7.48. Found: C, 68.33; H, 7.32; N, 7.38.

[NiCl(IPr)]₂(dppb) (2d). In a glovebox, $[(\mu\text{-Cl})(\text{IPr})\text{Ni}]_2$ (**1**; 0.05 mmol, 48 mg), dppb (0.05 mmol, 21 mg), and THF (0.5 mL) were added to a 5 mL screw-capped tube. After the compounds had dissolved, hexane (1.5 mL) was slowly added and the solution was cooled to $-30\text{ }^{\circ}\text{C}$. Yellow crystals of **2d** were obtained after removal of the liquid and washing with a small amount of hexane (63 mg, 91% yield). $^1\text{H NMR}$ (C_6D_6): δ 1.75 (bs), 4.55 (bs), 8.52 (bs), 10.78 (bs). Anal. Calcd (%) for $\text{C}_{45}\text{H}_{51}\text{N}_2\text{O}_3\text{PClNi}$: C, 70.76; H, 7.24; N, 4.03. Found: C, 70.06; H, 7.33; N, 3.77.

[NiCl(PPh₃)(IMes)] (3a). A solution of 1,3-bis(2,4,6-trimethylphenyl)imidazolium chloride [IMes/HCl] (428 mg, 1.26 mmol) and $\text{KN}(\text{SiMe}_3)_2$ (253 mg, 1.26 mmol) in THF (20 mL) was stirred for 3 h. The mixture was filtered through Celite and added to a mixture of $\text{Ni}(\text{cod})_2$ (158 mg, 0.57 mmol) and $\text{Ni}(\text{PPh}_3)_2\text{Cl}_2$ (374 mg, 0.57 mmol). The mixture was stirred at room temperature overnight to afford a dark yellow solution. The yellow solution was filtered through Celite, and the solvent was removed under vacuum. The yellow solid was recrystallized from toluene/hexane. Yield: 634 mg (84%). $^1\text{H NMR}$ (C_6D_6): δ 1.44 (bs), 3.24 (bs), 4.46 (bs), 8.26 (bs), 10.99 (bs). Anal. Calcd (%) for $\text{C}_{39}\text{H}_{39}\text{ClN}_2\text{NiP}$: C, 70.88; H, 5.95; N, 4.24. Found: C, 70.52; H, 5.97; N, 4.31.

[NiBr(PPh₃)(IMes)] (3b). A solution of 1,3-bis(2,4,6-trimethylphenyl)imidazolium chloride [IMes/HCl] (427 mg, 1.26 mmol) and $\text{KN}(\text{SiMe}_3)_2$ (256 mg, 1.26 mmol) in THF (20 mL) was stirred for 3 h. The mixture was filtered through Celite and added to a mixture of $\text{Ni}(\text{cod})_2$ (174 mg, 0.63 mmol) and $\text{Ni}(\text{PPh}_3)_2\text{Br}_2$ (461 mg, 0.63 mmol). The mixture was stirred at room temperature overnight to afford a dark yellow solution. The yellow solution was filtered through Celite, and the solvent was removed under vacuum. The yellow solid was recrystallized from THF/hexane. Yield: 440 mg (49%). $^1\text{H NMR}$ (C_6D_6): δ 1.51 (bs), 3.20 (bs), 4.35 (bs), 8.23 (d, $J = 8.6\text{ Hz}$, 4H), 10.94 (d, $J = 8.3\text{ Hz}$, 4H). Anal. Calcd (%) for $\text{C}_{47}\text{H}_{56}\text{BrN}_2\text{NiO}_2\text{P}$: C, 66.37; H, 6.64; N, 3.29; Found: C, 66.53; H, 6.41; N 3.30.

Triarylamine Synthesis via Buchwald–Hartwig Amination.

In a typical example, **1** (24.1 mg, 25 μmol) and ligand (300 μmol), di-*p*-(tolyl)amine (118.4 mg, 0.6 mmol), NaO^tBu (71.1 mg, 0.74 mmol), 4-bromobenzophenone (130.6 mg, 0.5 mmol), and THF (0.2 mL) were mixed and stirred at $40\text{ }^{\circ}\text{C}$ for 24 h. After addition of water, the organic layer was extracted three times with CH_2Cl_2 . The combined organic layers were washed with saturated $\text{NaCl}(\text{aq})$, dried with Na_2SO_4 , filtered, and concentrated in vacuo. The residue was purified by short column chromatography, with ethyl acetate/hexane (1:10) as the eluent, to give [4-[bis(4-methylphenyl)amino]phenyl]-phenylmethanone as a yellow oil. Yields: PPh_3 (186.9 mg, 99%), pyridine (184.9 mg, 98%), $\text{P}(\text{OPh})_3$ (73.6 mg, 39%).

Suzuki–Miyaura Cross-Coupling Reaction of Aryl Bromides with Phenylboronic Acid. In a typical example, an aryl bromide (0.15 mmol), phenylboronic acid (20 mg, 0.16 mmol, 1.1 equiv), a base (0.66 mmol, 4.4 equiv), and **3a** (11 mg, 15 μmol , 10 mol %) were dissolved in a solvent (1 mL). After stirring overnight at $80\text{ }^{\circ}\text{C}$ water was added. The organic layer was extracted with ethyl acetate. The combined organic layers were dried with Na_2SO_4 , filtered, and concentrated in vacuo to obtain white solids. The product was identified using NMR spectroscopy and GC-MS.

X-ray Crystallography of 2b–d, 3a, and 3b. Single crystals of **2b–d** and **3a,b** for X-ray diffraction were grown at $-30\text{ }^{\circ}\text{C}$ from the THF/hexane solutions. The data for **2b–d** and **3a,b** were obtained at 123 K using a Rigaku Saturn CCD diffractometer with a confocal mirror and graphite-monochromated $\text{Mo K}\alpha$ radiation ($\lambda = 0.71070\text{ \AA}$). Data reduction of the measured reflections was performed using the software package CrystalStructure.²² The structures were solved by direct methods (SIR2008)²³ and refined by full-matrix least-squares fitting based on F^2 , using the program SHELXL 97-2, PC version.²⁴ All non-hydrogen atoms were refined with anisotropic displacement parameters. All hydrogen atoms were located at ideal positions and included in the refinement, but were restricted to riding on the atom to which they were bonded. CCDC 1472756–1472760 contain the supplementary crystallographic data for this paper. A copy of the data can be obtained free of charge via <http://www.ccdc.cam.ac.uk/cgi-bin/catreq.cgi>.

DFT Calculations. All DFT calculations were performed using the Gaussian 09 package.²⁵ The B3LYP functional was used, with a standard split-valence basis set, 6-31G(d,p). The single-point calculations used to obtain SOMOs of **2a**, **2b**, **2c**, and **3a** were performed using crystallographic coordinates without geometry optimization and with a tight self-consistent field convergence criterion. All computations were performed using the computer facilities at the Research Institute for Information Technology, Kyushu University.

■ ASSOCIATED CONTENT

Supporting Information

The Supporting Information is available free of charge on the ACS Publications website at DOI: 10.1021/acs.organo-
met.6b00419.

Synthetic procedures, $^1\text{H NMR}$ spectra, elemental analysis, and SQUID for nickel complexes **2b–d** and **3a,b** (PDF)

■ AUTHOR INFORMATION

Corresponding Author

*E-mail (K. Matsubara): kmatsuba@fukuoka-u.ac.jp.

Author Contributions

The manuscript was written through contributions of all authors. All authors have given approval to the final version of the manuscript. Y.Y. conducted theoretical calculations, S.K. measured SQUID, and T.N. measured temperature-controlled ESR of the nickel(I) complexes. The other authors contributed equally.

Notes

The authors declare no competing financial interest.

■ ACKNOWLEDGMENTS

This work was supported by the Japan Society for the Promotion of Science (Grant-in-Aid for Scientific Research 22550104 and 25410123).

■ REFERENCES

- (1) (a) Tasker, S. Z.; Standley, E. A.; Jamison, T. F. *Nature* **2014**, *509*, 299–309. (b) Montgomery, J. In *Organometallics in Synthesis: Fourth Manual*; Lipshutz, B. H., Ed.; John Wiley & Sons: Hoboken, NJ, 2013; Chapter 3, pp 319–428. (c) *Modern Organonickel Chemistry*; Tamaru, Y., Ed.; Wiley-VCH: Weinheim, 2005. (d) Hassan, J.; Sévignon, M.; Gozzi, C.; Schulz, E.; Lemaire, M. *Chem. Rev.* **2002**, *102*, 1359–1469.
- (2) (a) Ford, L.; Jahn, U. *Angew. Chem., Int. Ed.* **2009**, *48*, 6386–6389. (b) Gao, C.-Y.; Cao, X.; Yang, L.-M. *Org. Biomol. Chem.* **2009**, *7*, 3922–3925. (c) Breitenfeld, J.; Ruiz, J.; Wodrich, M. D.; Hu, X. *J. Am. Chem. Soc.* **2013**, *135*, 12004–12012. (d) Ren, P.; Vechorkin, O.; von

Allmen, K.; Scopelliti, R.; Hu, X. *J. Am. Chem. Soc.* **2011**, *133*, 7084–7095. (e) Schley, N. D.; Fu, G. C. *J. Am. Chem. Soc.* **2014**, *136*, 16588–16593.

(3) (a) Chatani, N.; Tobisu, M. *Acc. Chem. Res.* **2015**, *48*, 1717–1726. (b) Weix, D. J. *Acc. Chem. Res.* **2015**, *48*, 1767–1775. (c) Liu, D.; Li, Y.; Qi, X.; Liu, C.; Lan, Y.; Lei, A. *Org. Lett.* **2015**, *17*, 998–1001. (d) Gutierrez, O.; Tellis, J. C.; Primer, D. N.; Molander, G. A.; Kozlowski, M. C. *J. Am. Chem. Soc.* **2015**, *137*, 4896–4899. (e) Biswas, S.; Weix, D. J. *J. Am. Chem. Soc.* **2013**, *135*, 16192–16197. (f) Anderson, T. J.; Jones, G. D.; Vivic, D. A. *J. Am. Chem. Soc.* **2004**, *126*, 8100–8101.

(4) (a) Miyazaki, S.; Koga, Y.; Matsumoto, T.; Matsubara, K. *Chem. Commun.* **2010**, *46*, 1932–1934. (b) Zhang, K.; Conda-Sheridan, M.; Cooke, S. R.; Louie, J. *Organometallics* **2011**, *30*, 2546–2552. (c) Page, M. J.; Lu, W. Y.; Poulten, R. C.; Carter, E.; Algarra, A. G.; Kariuki, B. M.; Macgregor, S. A.; Mahon, M. F.; Cavell, K. J.; Murphy, D. M.; Whittlesey, M. K. *Chem. - Eur. J.* **2013**, *19*, 2158–2167.

(5) (a) Jones, G. D.; Martin, J. L.; McFarland, C.; Allen, O. R.; Hall, R. E.; Haley, A. D.; Brandon, R. J.; Konovalova, T.; Desrochers, P. J.; Pulay, P.; Vivic, D. A. *J. Am. Chem. Soc.* **2006**, *128*, 13175–13183. (b) Lin, X.; Phillips, D. L. *J. Org. Chem.* **2008**, *73*, 3680–3688.

(6) (a) Kitiachvili, K. D.; Mendiola, D. J.; Hillhouse, G. L. *J. Am. Chem. Soc.* **2004**, *126*, 10554–10555. (b) Melenkivitz, R.; Mendiola, D. J.; Hillhouse, G. L. *J. Am. Chem. Soc.* **2002**, *124*, 3846–3847. (c) Holland, P. L.; Cundari, T. R.; Perez, L. L.; Eckert, N. A.; Lachicotte, R. J. *J. Am. Chem. Soc.* **2002**, *124*, 14416–14424. (d) Eckert, N. A.; Dinescu, A.; Cundari, T. R.; Holland, P. L. *Inorg. Chem.* **2005**, *44*, 7702–7704. (e) Fujita, K.; Rheingold, A. L.; Riordan, C. G. *Dalton Trans.* **2003**, 2004–2008. (f) Eaborn, C.; Hill, M. S.; Hitchcock, P. B.; Smith, J. D. *Chem. Commun.* **2000**, 691–692. (g) Ito, M.; Matsumoto, T.; Tatsumi, K. *Inorg. Chem.* **2009**, *48*, 2215–2223. (h) Marlier, E. E.; Tereniak, S. J.; Ding, K.; Mulliken, J. E.; Lu, C. C. *Inorg. Chem.* **2011**, *50*, 9290–9299. (i) Laskowski, C. A.; Bungum, D. J.; Baldwin, S. M.; Ciello, S. A. D.; Iluc, V. M.; Hillhouse, G. L. *J. Am. Chem. Soc.* **2013**, *135*, 18272–18275.

(7) Dible, R. B.; Arif, M. A.; Sigman, S. M. *Inorg. Chem.* **2005**, *44*, 3774–3776.

(8) Nagao, S.; Matsumoto, T.; Koga, Y.; Matsubara, K. *Chem. Lett.* **2011**, *40*, 1036–1038.

(9) Sanford, M. S.; Love, J. A.; Grubbs, R. H. *J. Am. Chem. Soc.* **2001**, *123*, 6543–6554.

(10) (a) *N-Heterocyclic Carbenes*; Nolan, S. P., Ed.; Wiley-VCH: Weinheim, 2014. (b) Hopkinson, N. M.; Richter, C.; Schedler, M.; Glorius, F. *Nature* **2014**, *510*, 485–496. (c) Nelson, J. D. *Eur. J. Inorg. Chem.* **2015**, 2015, 2012–2027.

(11) Davies, C. J. E.; Page, M. J.; Ellul, C. E.; Mahon, M. F.; Whittlesey, M. K. *Chem. Commun.* **2010**, *46*, 5151–5153.

(12) (a) Matsubara, K.; Ueno, K.; Shibata, Y. *Organometallics* **2006**, *25*, 3422–3427. (b) Liu, Z.-H.; Xu, Y.-C.; Xie, L.-Z.; Sun, H.-M.; Shen, Q.; Zhang, Y. *Dalton Trans.* **2011**, *40*, 4697–4706.

(13) Lejkowski, L. M.; Lindner, R.; Kageyama, T.; Bodizs, E. G.; Plessow, N. P.; Muller, B. I.; Schafer, A.; Rominger, F.; Hofmann, P.; Futter, C.; Schunk, A. S.; Michael, L. *Chem. - Eur. J.* **2012**, *18*, 14017–14025.

(14) (a) Bricout, H.; Carpentier, J.-F.; Mortreux, A. *Tetrahedron Lett.* **1997**, *38*, 1053–1056. (b) Bricout, H.; Carpentier, J.-F.; Mortreux, A. *Tetrahedron* **1998**, *54*, 1073–1084. (c) Edwards, J. A.; Retbüll, M.; Wenger, E. *Acta Crystallogr., Sect. E: Struct. Rep. Online* **2002**, *58*, 375–377. (d) Retbüll, M.; Edwards, J. A.; Rae, A. D.; Willis, C. A.; Bennett, A. M.; Wenger, E. *J. Am. Chem. Soc.* **2002**, *124*, 8348–8360. (e) Fischer, R.; Langer, J.; Malassa, A.; Walther, D.; Gorls, H.; Vaughan, G. *Chem. Commun.* **2006**, 2510–2512.

(15) Serron, S. A.; Aldridge, W. S., III; Fleming, C. N.; Danell, R. M.; Baik, M.-H.; Sykora, M.; Dattelbaum, D. M.; Meyer, T. J. *J. Am. Chem. Soc.* **2004**, *126*, 14506–14514.

(16) Because identification of each signal in the NMR spectra of the paramagnetic compounds **2** was difficult, the values of the ratios between **1** and **2** were not determined.

(17) For example, see: Kogut, E.; Wiencko, H. L.; Zhang, L.; Cordeau, D. E.; Warren, T. H. *J. Am. Chem. Soc.* **2005**, *127*, 11248–11249.

(18) (a) Han, F.-S. *Chem. Soc. Rev.* **2013**, *42*, 5270–5298. (b) Maluenda, L.; Navarro, O. *Molecules* **2015**, *20*, 7528–7557.

(19) (a) Wolfe, J. P.; Wagaw, S.; Marcoux, J.-F.; Buchwald, S. T. *Acc. Chem. Res.* **1998**, *31*, 805–818. (b) Hartwig, J. F. *Acc. Chem. Res.* **2008**, *41*, 1534–1544.

(20) Jafarpour, L.; Stevens, E. D.; Nolan, S. P. *J. Organomet. Chem.* **2000**, *606*, 49–54.

(21) Matsubara, K.; Miyazaki, S.; Koga, Y.; Nibu, Y.; Hashimura, T.; Matsumoto, T. *Organometallics* **2008**, *27*, 6020–6024.

(22) *CrystalStructure 4.0: Crystal Structure Analysis Package*; Tokyo 196-8666, Japan, 2000–2011.

(23) SIR2008: Burla, M. C.; Caliandro, R.; Camalli, M.; Carrozzini, B.; Cascarano, G. L.; De Caro, L.; Giacovazzo, C.; Polidori, G.; Siliqi, D.; Spagna, R. *J. Appl. Crystallogr.* **2007**, *40*, 609–613.

(24) Sheldrick, G. M. *SHELXL97*; University of Gottingen: Germany, 1997.

(25) Frisch, M. J.; Trucks, G. W.; Schlegel, H. B.; et al. *Gaussian 09*, Revision D.01; Gaussian, Inc.: Wallingford, CT, 2013.